

# VALENCE ELECTRONIC STATE DENSITY IN THORIUM DIOXIDE

by

Anton YU. TETERIN<sup>1</sup>, Mikhail V. RYZHKOV<sup>2</sup>, Yury A. TETERIN<sup>1</sup>, Labud VUKČEVIĆ<sup>3</sup>,  
Vladimir A. TEREKHOV<sup>4</sup>, Konstantin I. MASLAKOV<sup>1</sup>, and Kirill E. IVANOV<sup>1</sup>

Received on July 23, 2008; accepted on October 2, 2008

This work analyses the fine low energy (0-40 eV) X-ray photoelectron spectra of ThO<sub>2</sub>, taking into account relativistic X<sub>α</sub>-discrete variation electronic structure calculations for the ThO<sub>8</sub><sup>12-</sup> (D<sub>4h</sub>) cluster reflecting thorium's close environment in ThO<sub>2</sub>. As a result, it was theoretically shown and experimentally confirmed that Th5f electrons in ThO<sub>2</sub> can participate directly (0.6 Th5f electrons) in chemical bond formation. Th6p electrons were shown to be a significant part (0.44 Th6p electrons) not only of inner valence molecular orbitals, but to play a significant role in outer valence molecular orbitals formation, as well. Inner valence molecular orbitals composition and sequent order were established to belong to the binding energy range of 13 eV to 40 eV. The valence electronic state density in the range of 0-40 eV in ThO<sub>2</sub> was also calculated. For the first time, these data allowed an interpretation of the fine X-ray photoelectron spectra (0-40 eV) and high resolution O<sub>4,5</sub>(Th) X-ray emission spectral structure (60 – 85 eV) of ThO<sub>2</sub>.

*Key words: X-ray photoelectron spectra, thorium oxide, outer and inner valence molecular orbitals*

## INTRODUCTION

While studying X-ray photoelectron spectra (XPS) from thorium oxide in the 0-40 eV binding energy range, the observed lines were found to be several eV wide, which was wider than some corresponding core lines [1]. For instance, the O1s ( $E_b = 530.2$  eV) line in the spectrum from ThO<sub>2</sub> is 1.4 eV wide, while the corresponding O2s line ( $E_b \sim 22.0$  eV) is observed to be more than 4 eV wide and structured [1]. It contradicts the uncertainty ratio  $\Delta E \Delta \tau \sim h/2\pi$ , where  $h$  is the

Plank's constant, the natural width of the level from which an electron was removed, and  $\Delta E$  – the inversely proportional to the lifetime  $\Delta \tau$  of the formed ion ("hole"). Indeed, since the lifetime of the "hole" ( $\Delta \tau$ ) decreases while the absolute energy of the atomic level increases, the XPS lines of low-energy levels must be narrower for atoms. In the case of ThO<sub>2</sub> and other actinide oxides, the picture was reversed. This caused intense theoretical and experimental studies of the nature of the chemical bond in actinide compounds. One of the reasons of the observed widening of the low-energy (0-40 eV) spectral lines of thorium dioxide is the formation of the outer valence molecular orbitals (OVMO) – 0-13 eV binding energy, and inner valence molecular orbitals (IVMO) – 13-40 eV binding energy, molecular orbitals with effective participation of An6p filled atomic shells [2, 3]. Practically, these spectra reflect the valence band structure (0-40 eV), and are observed as several eV wide bands. Furthermore, it was shown that, under certain conditions, IVMO can form in compounds of any elements of the periodic table [3].

Despite the fact that atomic thorium does not have Th5f electrons, some experimental [4, 5] and relativistic and non-relativistic theoretical [6] results show the presence of filled Th5f states in the valence band of thorium oxide, which suggests the participation of Th5f atomic shells in the formation of molecular orbitals. This principally novel fact needs to be yet confirmed.

Nuclear Technology & Radiation Protection  
Scientific paper

UDC: 546.795:535.333:543.428.4

BIBLID: 1451-3994, 23 (2008), 2, pp. 34-42

DOI: 10.2298/NTRP0802034T

Authors' addresses:

<sup>1</sup> Russian Research Centre "Kurchatov Institute"  
Kurchatov square, Moscow 123182, Russia

<sup>2</sup> Institute of Solid State Chemistry of Ural Dept. of RAS  
91, Pervomaiskaya Str., GSP-145  
620041 Ekaterinburg, Russia

<sup>3</sup> Faculty of Natural Sciences and Mathematics  
University of Montenegro  
P. O. Box 211, Podgorica, Montenegro

<sup>4</sup> Voronezh State University  
1, University square  
394006 Voronezh, Russia

E-mail address of corresponding author:  
teterin@ignph.kiae.ru (Yu. A. Teterin)

The data of the qualitative interpretation of XPS of  $\text{ThO}_2$  [1], taking into account the non-relativistic calculation results, allowed a preliminary identification of the high-resolution  $\text{O}_{4,5}(\text{Th})$  X-ray emission spectral (XES) structure [7]. The absence of relativistic calculation results hampered a correct interpretation of fine XPS and  $\text{O}_{4,5}(\text{Th})$  XES spectral structures.

This work analyses the fine low energy (0-40 eV) XPS and high-resolution  $\text{O}_{4,5}(\text{Th})$  XES spectra of  $\text{ThO}_2$ , taking into account the relativistic  $X_\alpha$ -discrete variation ( $\text{RX}_\alpha$ -DVM) electronic structure calculations for the  $\text{ThO}_8^{12-}(\text{D}_{4h})$  cluster reflecting thorium's close environment in  $\text{ThO}_2$ .

## EXPERIMENTAL

XPS spectra of  $\text{ThO}_2$  were measured with an electrostatic spectrometer HP5950A, using monochromatized  $\text{AlK}_{\alpha,1,2}$  ( $h\nu = 1486.6$  eV) radiation under  $1.3 \cdot 10^{-7}$  Pa at room temperature. The device resolution was 0.8 eV measured as full width on the half-maximum (FWHM) of the  $\text{Au}4f_{7/2}$  line on the standard rectangular gold plate. The binding energies  $E_b$  (eV) were measured relatively to the binding energy of the C1s electrons from hydrocarbons adsorbed on the sample surface, accepted to be equal to 285.0 eV. For the gold standard, the calibration binding energies  $E_b(\text{C1s}) = 284.7$  eV and  $E_b(\text{Au}4f_{7/2}) = 83.8$  eV [1] were used. The O1s XPS from  $\text{ThO}_2$  was observed as a single, 1.4 eV wide peak, while the C1s XPS from the surface hydrocarbons was 1.3 eV wide.

The  $\text{ThO}_2$  sample for the XPS study was prepared from the finely dispersed powder ground in agate mortar as a dense thick layer with a flat surface pressed in indium on a metal substrate. The XPS parameters of the sample (binding energies) within the measurement error did not differ from the standard values for  $\text{ThO}_2$  formed on the metallic thorium plate [8]. The elastic scattering related spectral background was subtracted by Shirley [9].

The  $\text{O}_{4,5}(\text{Th})$  XES reflecting the  $\text{Th}6p$  and  $\text{Th}7p,5f$  states in the valence band was measured by the primary procedure with a RSM-500 spectrometer with an energy resolution of 0.3 eV [7] at the voltage on the X-ray tube of 3 kV (2 mA) during 60 minutes. The variation in the energy of excitation electrons allowed for a change in the effective measurement depth from 15 nm to 50 nm. The area of the excitation electron spot was  $5 \cdot 5 \text{ mm}^2$ . The sample was ground into the agate mortar and as a powder pressed into a grooved silver plate attached to the X-ray anode. A secondary electronic multiplier, VEU-1, was used for spectra registration. A CsI film was used as a photocathode with the quantum yield within the analysed spectral range. To exclude the influence of the composition change effect under the electron beam, the  $\text{O}_{4,5}(\text{Th})$  spectrum was collected three times. The

lines of Zr (75.55 eV) and Nb (85.85 eV) were used for energy calibration in the second reflection order M.

The  $\text{ThO}_8^{12-}(\text{D}_{4h})$  cluster reflecting thorium's close environment in  $\text{ThO}_2$  is a body-centered cube with Th inside and oxygens in the corners with an interatomic distance of  $R_{\text{Th-O}} = 2.425 \cdot 10^{-10}$  m [10]. In this work, the calculations were done for the first time in the  $\text{RX}_\alpha$ -DVM [11, 12], based on the Dirack-Slater equation solution for 4-component spinors with exchange-correlation potential [13]. The extended basis of the numeric atomic orbitals from the Dirack-Slater equation solution for isolated atoms included vacant  $\text{Th}5f, 7p_{1/2}, 7p_{3/2}$  states besides the filled ones. The basis also took into account cluster symmetry, *i. e.* linear combinations converted by the irreducible representations of the binary  $\text{D}_{4h}$  group were constructed from regular atomic orbitals (AO), using the technique of projecting operators [11]. To obtain the relativistic basis, an original symmetrization program was used [13-15]. The numeric Diophantine integration for the calculation of matrix elements of the secular equation was done by a number of 22 000 points distributed in the cluster space. It provided the convergence of molecular orbitals (MO) energies of not less than 0.1 eV. The local exchange-correlation potential was taken in form of  $X_\alpha$  with  $\alpha$  equal to the mean atomic values. Since the clusters were fragments of a crystal, the renormalization of the ligand valence MO population was done during self-consistency. It allowed us to effectively take into account the stoichiometry and charge redistribution between the ligands and the surrounding crystal.

## RESULTS AND DISCUSSION

The low binding energy (0-40 eV) XPS from  $\text{ThO}_2$  can be conditionally subdivided into two ranges (fig. 1). The first one, 0-13 eV, exhibits the OVMO related structure formed from the not completely filled valence  $\text{Th}6d, 7s, 5f, 7p$  and  $\text{O}2p$  AOs (tab. 1). The sec-

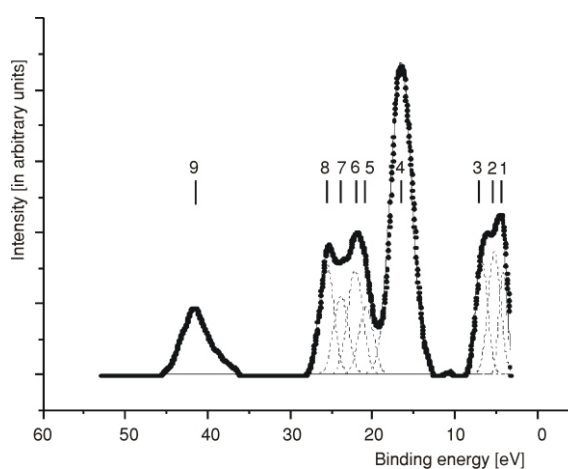


Figure 1. XPS from  $\text{ThO}_2$ , separation into individual components is shown

**Table 1. Compositions and MO energies  $E_0$  of the  $\text{ThO}_8^{12-}(\text{O}_h)$  cluster at  $R_{\text{Th-O}} = 2.425 \cdot 10^{-10}$  m (RX $\alpha$ -DVM) and photoionization cross-sections  $\sigma_i$** 

MO	$-E_0$ [eV]	MO composition														
		Th										O				
		$\sigma_1^{(a)}$	6s	6p <sub>1/2</sub>	6p <sub>3/2</sub>	6d <sub>3/2</sub>	6d <sub>5/2</sub>	7s	5f <sub>5/2</sub>	5f <sub>7/2</sub>	7p <sub>1/2</sub>	7p <sub>3/2</sub>	2s	2p <sub>1/2</sub>	2p <sub>3/2</sub>	
			1.09	0.89	1.24	0.79	0.74	0.13	2.74	2.56	0.07	0.09	0.96	0.07	0.07	
OVMO	22 $\gamma$	-11.47					0.82						0.05	0.09	0.04	
	25 $\gamma_6$	-11.15				0.44	0.38						0.04	0.02	0.12	
	21 $\gamma$	-11.15				0.44	0.38						0.04	0.03	0.11	
	24 $\gamma$	-9.27							0.19	0.73			0.01	0.03	0.04	
	28 $\gamma_6$	-9.10								0.50	0.43		0.04	0.01	0.02	
	24 $\gamma_6$	-8.70						0.87					0.07	0.02	0.04	
	27 $\gamma_6$	-8.44							0.04	0.86		0.07	0.01	0.01	0.01	
	23 $\gamma$	-8.43							0.04	0.85		0.06	0.01	0.01	0.03	
	22 $\gamma$	-7.91							0.76	0.21				0.01	0.02	
	26 $\gamma_6$	-7.90							0.78	0.08		0.10	0.01	0.01	0.02	
	21 $\gamma$	-7.90							0.78	0.08		0.09	0.01		0.04	
	25 $\gamma_6$	-7.69								0.45	0.47		0.01	0.06	0.01	
	23 $\gamma_6$	-7.39				0.39	0.46							0.05	0.10	
	20 $\gamma$	-7.37				0.39	0.46							0.05	0.10	
	24 $\gamma_6$	-7.15							0.14	0.02		0.75	0.02		0.07	
	20 $\gamma$	-7.11							0.12	0.02		0.77	0.02		0.07	
	OVMO	19 $\gamma^-$ (b)	0.00			0.09				0.02	0.01				0.29	0.59
		23 $\gamma_6$	0.00			0.09				0.02	0.01				0.15	0.73
		22 $\gamma_6$	0.26												0.34	0.66
		18 $\gamma$	0.26												0.34	0.66
22 $\gamma_6$		0.45												0.15	0.85	
19 $\gamma$		0.45												0.15	0.85	
21 $\gamma_6$		0.47												0.64	0.34	
21 $\gamma_6$		0.68		0.01						0.03				0.75	0.21	
18 $\gamma$		0.72					0.01							0.05	0.94	
17 $\gamma$		0.74				0.01								0.49	0.50	
20 $\gamma_6$		0.74				0.01								0.48	0.51	
17 $\gamma$		0.85							0.03	0.04				0.30	0.63	
16 $\gamma$		1.23			0.01				0.01	0.01		0.05		0.15	0.77	
20 $\gamma_6$		1.24			0.01				0.01	0.01		0.05		0.08	0.84	
19 $\gamma_6$		1.48		0.01						0.01	0.05			0.41	0.52	
19 $\gamma_6$		1.91	0.01										0.01	0.32	0.60	
15 $\gamma$		2.00							0.01	0.02				0.19	0.78	
18 $\gamma_6$		2.00							0.01	0.02				0.17	0.80	
14 $\gamma$		2.01							0.02	0.02				0.62	0.34	
16 $\gamma$		2.17				0.01	0.11						0.01	0.51	0.36	
18 $\gamma_6$	2.19				0.07	0.05						0.01	0.03	0.84		
15 $\gamma$	2.19				0.06	0.05						0.01	0.35	0.53		
14 $\gamma$	2.81				0.06	0.09							0.28	0.57		
17 $\gamma_6$	2.82				0.06	0.09							0.28	0.57		
IVMO	17 $\gamma_6$	10.54			0.76							0.01	0.13	0.02	0.08	
	13 $\gamma$	10.54			0.76							0.01	0.13	0.04	0.06	
	16 $\gamma_6$	14.95		0.16							0.04		0.80			
	12 $\gamma$	15.16							0.01	0.01			0.98			
	16 $\gamma_6$	15.54				0.03	0.02						0.95			
	13 $\gamma$	15.54				0.01	0.04						0.95			
	12 $\gamma$	15.54				0.02	0.04						0.94			
	15 $\gamma_6$	15.94	0.01					0.07					0.92			
	11 $\gamma$	16.39			0.14				0.01	0.01		0.02	0.82			
	15 $\gamma_6$	16.32			0.14						0.02	0.02	0.84			
14 $\gamma_6$	19.06			0.82						0.01		0.15	0.01	0.01		
14 $\gamma_6$	34.40		0.98									0.01		0.01		

<sup>(a)</sup> photoionization cross-sections  $\sigma_i$  ( $10^{-25}$  m<sup>2</sup> per one electron) calculated by V. G. Yarzhevsky<sup>(b)</sup> upper filled MO (2 electrons), filling number for all orbitals is 2

ond one, 13-40 eV, shows the IVMO related structure formed due to the strong interaction of the completely filled inner Th6p and O2s AOs. The OVMO structure has some typical features and can be subdivided into four components (1-4). The IVMO XPS shows explicit peaks and can be subdivided into five components (5-9) (fig. 1). Although this subdivision is formal, it allows a qualitative and quantitative comparison of XPS parameters with theoretical calculation results for the  $\text{ThO}_8^{12-}(\text{D}_{4h})$  cluster.

Relativistic calculation results for the ground state of the  $\text{ThO}_8^{12-}(\text{D}_{4h})$  cluster and MO composition are given in tab. 1. Since, in the excited state, electron photoemission results with a hole on some of the levels, for a more strict comparison of experimental and theoretical binding energies, the calculations were performed for the transition state [16]. However, within a certain approximation, one can suggest that, for the valence band, the binding energies calculated for the transition state differ from those of the ground state by a constant shift toward higher binding energies. Therefore, in this work, corresponding theoretical binding energies were increased by 5.96 eV (tab. 2). Taking into account MO compositions (tab. 1) and photoionization cross-sections [17],  $\sigma_1$  for Th in tab. 1, were calculated by prof. V. G. Yarzhemsky and theoretical intensities for some of the spectral ranges determined (tab. 2). Comparing experimental XPS and theoretical data, one has to take into account that the XPS from  $\text{ThO}_2$  reflects the band structure and consists of bands widened due to the solid-state effects. Despite calculation errors, a satisfactory qualitative agreement between the theoretical and experimental results was observed. Indeed, corresponding theoretical and experimental relative intensities and widths of the inner and outer valence bands are comparable. Also, a satisfactory agreement between the experimental and calculated binding energies for some levels was reached (tab. 2). The worst discrepancy was observed for the middle IVMO part ( $12\gamma_7-15\gamma_6$ ). Earlier, the non-relativistic  $X_\alpha$ -DVM results were used for interpretation of the IVMO range XPS from  $\text{ThO}_2$  [1, 18]. It allowed a qualitative identification of the fine spectral structure only in the binding energy range of 0-20 eV, because the O2s AO by the binding energy are located somewhere around the middle of Th $6_{3/2}$  and Th $6_{1/2}$  electronic shells. Therefore, non-relativistic calculations could not allow even for a qualitative interpretation of the IVMO structure in  $\text{ThO}_2$ . Taking into account relativistic effects, the results of the present work allow an identification of XPS from  $\text{ThO}_2$  over the whole range of 0-40 eV.

Thus, the intensity of the outer valence band predominantly comes from the outer valence Th5f,6d,7s,7p and O2p AOs, and to a lesser degree, from the inner valence Th6p and O2s AOs. Th5f electrons contribute significantly to OVMO intensity (tabs. 1 and 2), since the Th5f photoionization

cross-section is pretty high (tab. 1). The authors of [5] have shown that, without taking into account the participation of Th5f electrons in the chemical bond in  $\text{ThO}_2$ , the calculated OVMO/IVMO intensity ratio is 0.20, much lower than the corresponding experimental value of 0.35. Taking the Th5f participation in the chemical bond into account, yields an OVMO/IVMO intensity ratio of 0.4, which is in a qualitative agreement with the experimental value (tab. 2). Practically, direct participation of Th5f electrons in the formation of the chemical bond without the loss of their f-nature was experimentally confirmed. Th5f states by the binding energy are close to the top and middle of the outer valence band (tab. 1). Th6d states are located at the bottom of the outer valence band.

In the IVMO XPS range, a satisfactory agreement was reached; for example, for the  $17\gamma_6$ ,  $13\gamma_7$  (4), and  $14\gamma_6$  (8) IVMOs determining the band width for these orbitals. It has to be noted that theoretical and experimental total relative OVMO and IVMO intensities are comparable, which is in favour of the approximation chosen for these calculations (tab. 2). The calculated and experimental relative IVMO intensities, except for the  $16\gamma_6$  IVMO, are practically in weak agreement.

Taking into account relativistic calculations data for the  $\text{ThO}_8^{12-}(\text{D}_{4h})$  cluster and experimental core and outer levels binding energy differences [19] in the MO LCAO (molecular orbitals as linear combinations of atomic orbitals) approximation, one can build a MO scheme for this cluster (fig. 2). The scheme provides an understanding of the real XPS structure of  $\text{ThO}_2$ . In this approximation, one can separate the antibonding  $17\gamma_6$ ,  $13\gamma_7$ (4), and  $16\gamma_6$ (5), as well as the corresponding bonding  $15\gamma_6$ ,  $11\gamma_7$ (7), and  $14\gamma_6$ (8) IVMOs, and also the quasiautomatic  $12\gamma_7$ ,  $16\gamma_6$ ,  $13\gamma_7$ ,  $12\gamma_7$ , and  $15\gamma_6$ (6) IVMOs, basically related to O2s electrons. This experimental data shows that the binding energies of the quasiautomatic IVMOs related, basically, with the O2s AOs must be close in magnitude. Indeed, the O1s XPS from  $\text{ThO}_2$  allows us to evaluate that their chemical non-equivalence must not exceed 0.1 eV, since this peak was observed symmetric and 1.4 eV wide. The O2s binding energy must be 22.2 eV, since  $\Delta E_O = 508.0$  eV, while the O1s binding energy in  $\text{ThO}_2$  is  $E_b = 530.2$  eV (fig. 2). These data partially agree with the theoretical calculation results. Taking into account that  $\Delta E_{\text{Th}} = 316.5$  eV,  $\Delta E_1 = 317.8$  eV, one can find  $\Delta_1 = 1.3$  eV [3]. Since the  $17\gamma_6$ ,  $13\gamma_7$ (4) and  $14\gamma_6$ (8) IVMO binding energy difference is 9.1 eV, and the Th6p spin-orbit splitting in atomic Th is  $\Delta E_{\text{sl}}(\text{Th6p}) = 9.2$  eV (calculated [20]) and  $\Delta E_{\text{sl}}(\text{Th6p}) = 9.3$  eV (experimental [19]), one can evaluate the disturbance  $\Delta_1 = 0.2$  eV, which does not agree with the corresponding value of 1.3 eV found at the core – valence band binding energy distance. Such a difference can be explained by IVMO formation, although this comparison may not be sufficiently correct. The IVMO FWHM does not allow us to reach a conclusion about the nature

of orbitals (bonding or antibonding). However, one can suggest that the 10% admixture of O2p and 1% of Th7p AOs to the  $17\gamma_6$ ,  $13\gamma_7$  (4) IVMOs make these orbitals partially loose their antibonding nature (tabs. 1 and 2, fig. 2, [3]).

Experimental evidence of IVMO formation in ThO<sub>2</sub> is the O<sub>4,5</sub>(Th) XES structure (fig. 3). Previously,

this structure was interpreted on the basis of non-relativistic calculation results [1]. In this work, the O<sub>4,5</sub>(Th) XES structure was interpreted on the basis of XPS data for ThO<sub>2</sub> and relativistic calculation data for the ThO<sub>8</sub><sup>12-</sup>(D<sub>4h</sub>) cluster (tab. 3).

The considered XES [7, 21] reflecting Th<sub>5/2,3/2</sub> Th6p<sub>3/2,1/2</sub>, 7p, 5f [O<sub>4,5</sub>(Th) P<sub>2,3</sub>O<sub>VI</sub>(Th)] elec-

**Table 2. Parameters of the XPS from ThO<sub>2</sub> and ThO<sub>8</sub><sup>12-</sup> (O<sub>h</sub>) cluster at  $R_{\text{Th-O}} = 2.425 \cdot 10^{-10}$  m (RX<sub>α</sub>-DVM) and the Th6p- and Th5f-electron state density  $\rho_i$  (e<sup>-</sup>)**

MO		$-E^{(c)}$ [eV]	XPS			Th6p- and Th5f-electron state density $\rho_i$ (e <sup>-</sup> ), e <sup>-</sup>			
			Energy <sup>(d)</sup> [eV]	Intensity, [%]		5f <sub>5/2</sub>	5f <sub>7/2</sub>	6p <sub>1/2</sub>	6p <sub>3/2</sub>
				Experiment	Theory				
OVMO	$19\gamma_7^{-(a)}$	5.96	4.1 (1.2)	2.9	5.4	0.04	0.02		0.18
	$23\gamma_6^-$	5.96	5.2 (1.8)	2.9	9.7	0.04	0.02		0.18
	$22\gamma_6^-$	6.22		0.2					
	$18\gamma_7^-$	6.22		0.2					
	$22\gamma_6^+$	6.41		0.2					
	$19\gamma_7^+$	6.41		0.2					
	$21\gamma_6^+$	6.86	6.8 (1.8)	0.2	9.2				
	$21\gamma_6^-$	6.64		1.5			0.06	0.02	
	$18\gamma_7^+$	6.68		0.4					
	$17\gamma_7^+$	6.70		0.4					
	$20\gamma_6^+$	6.70		0.4					
	$17\gamma_7^-$	6.81		2.8		0.06	0.08		
	$16\gamma_7^-$	7.19		1.2		0.02	0.02		0.02
	$20\gamma_6^-$	7.20		1.2		0.02	0.02		0.02
	$19\gamma_6^-$	7.44		0.8			0.02	0.02	
	$19\gamma_6^+$	7.87		0.5					
	$15\gamma_7^-$	7.96		1.3		0.02	0.04		
	$18\gamma_6^-$	7.96		1.3		0.02	0.04		
	$14\gamma_7^-$	7.97		1.7		0.04	0.04		
	$16\gamma_7^+$	8.13		1.5					
$18\gamma_6^+$	8.15		1.5						
$15\gamma_7^+$	8.15		1.5						
$14\gamma_7^+$	8.77	10.8 (0.7)	1.8	0.1					
$17\gamma_6^+$	8.78		1.8						
	$\Sigma I_i^{(b)}$			28.4	24.4	0.26	0.36	0.04	0.40
IVMO	$17\gamma_6^-$	16.50	16.5 (3.0)	13.6	41.4				1.52
	$13\gamma_6^-$	16.50		13.6					1.52
	$16\gamma_6^-$	20.91	20.8 (2.1)	4.7	6.3			0.32	
	$12\gamma_6^-$	21.12		4.0		0.02	0.02		
	$16\gamma_6^+$	21.50		3.7					
	$13\gamma_6^+$	21.50	22.1 (2.3)	3.7	10.1				
	$12\gamma_6^+$	21.50		3.8					
	$15\gamma_6^+$	21.90		3.4					
	$11\gamma_6^-$	22.35	23.8 (2.1)	5.9	7.3	0.02	0.02		0.28
	$15\gamma_6^-$	22.28		5.0					0.28
	$14\gamma_6^-$	25.02	25.6 (2.2)	10.2	10.7			1.64	
		$\Sigma I_i^{(b)}$		71.6	75.6	0.04	0.04	1.96	3.60
	$14\gamma_6^+$	40.36	41.7(3.8)	11.9	10.5				

(a) Upper filled MO (2 electrons), filling number for all orbitals is 2

(b) Total Th6p electron state densities and peak intensities

(c) Energies are shifted toward the higher values (down) by 5.96 eV

(d) Peak widths [eV] are given in parentheses

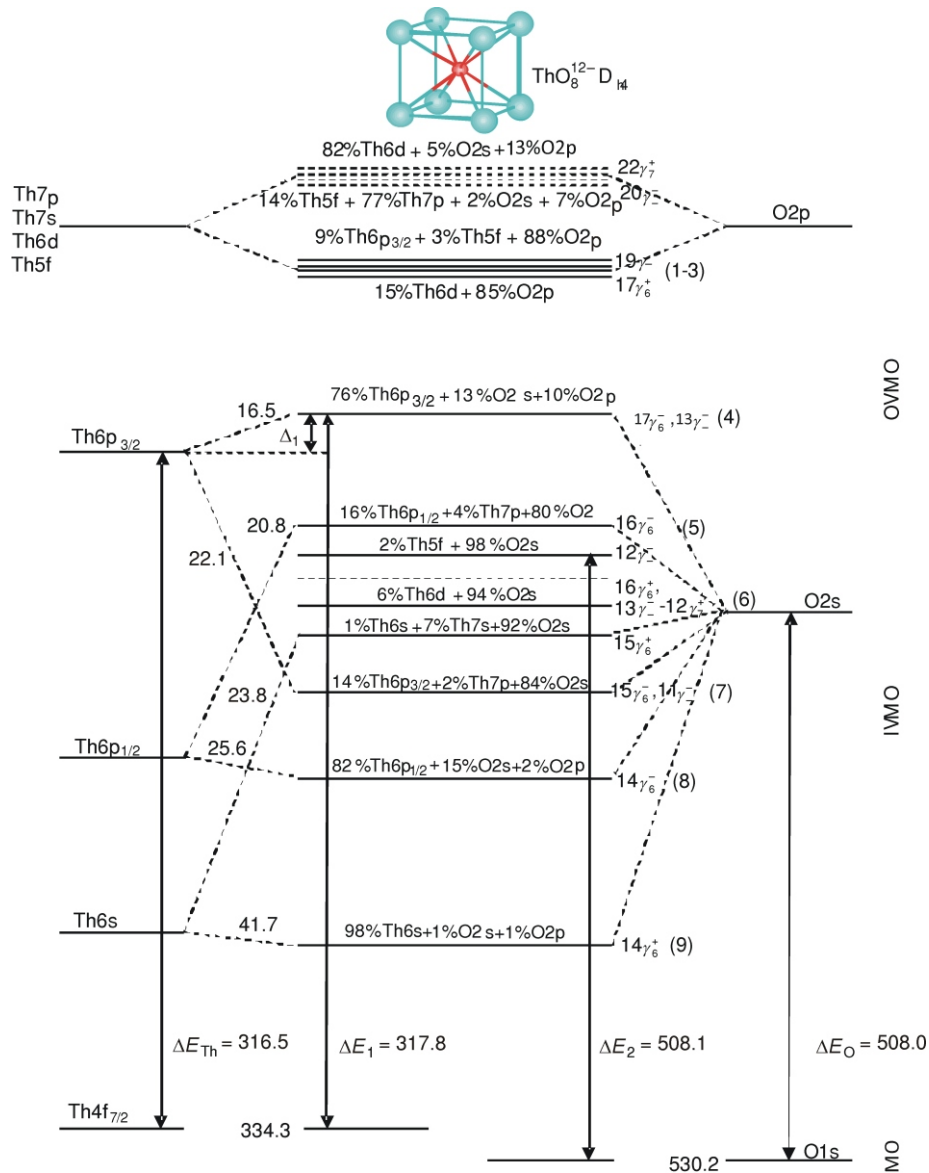
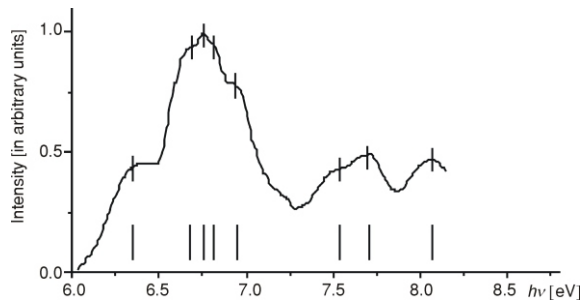


Figure 2. MO scheme for the  $\text{ThO}_8^{12-} (\text{D}_{4h})$  cluster built on the basis of theoretical and experimental data; chemical shifts are not shown; some of the experimentally measurable binding energy differences are shown as arrows; experimental binding energies [eV] are given to the left; energy scale is not kept

Table 3. X-ray  $\text{O}_{4,5}(\text{Th})$  emission  $\text{Th}5d \rightarrow \text{Th}6p, np$  transitions in Th and  $\text{ThO}_2$  (given in eV) by XPS and XES

Th		$\text{ThO}_2$		
Transition	XPS	Transition <sup>(a)</sup>	XPS	XES
$5d_{3/2} \rightarrow 6p_{1/2}$	68.0	$5d_{3/2} \rightarrow 15\gamma_6^-, 11\gamma_7^- (7)$	62.5	63.5
		$5d_{3/2} \rightarrow 14\gamma_6^- (8)$	67.7	67.6
$5d_{3/2} \rightarrow 6p_{3/2}$	68.8	$5d_{3/2} \rightarrow 17\gamma_6^-, 13\gamma_7^- (4)$	69.8	69.5
		$5d_{3/2} \rightarrow 15\gamma_6^-, 11\gamma_7^- (7)$	69.5	69.5
		$5d_{3/2} \rightarrow 16\gamma_6^-, (5)$	72.5	75.4
$5d_{3/2} \rightarrow 6p_{3/2}$	75.9	$5d_{3/2} \rightarrow 17\gamma_6^-, 13\gamma_7^- (4)$	76.8	77.0
		$5d_{3/2} \rightarrow \text{OVMO}$	80.5	80.7
		$5d_{3/2} \rightarrow \text{OVMO}$	87.5	

(a) Data for the  $\text{ThO}_8^{12-} (\text{D}_{4h})$  cluster



**Figure 3. X-ray  $O_{4,5}(\text{Th})$  emission spectrum reflecting the Th5d Th6p,7p transitions in  $\text{ThO}_2$  measured at 3 kV (2mA) [7, 21]**

tronic transitions in the energy range of  $60 < h\nu < 85$  eV in the short-wave region overlap with the absorption spectra [22] which can lead to a distortion, due to the self-absorption effect (fig. 3). Earlier [22], on the basis of XES data, the long-wave peak group was attributed to the transition triplet between the core levels in Th Th5d<sub>5/2,3,2</sub>

Th6p<sub>3/2,1/2</sub>, [ $O_{4,5}(\text{Th})$  P<sub>2,3</sub>(Th)] (fig. 3, tab. 3). However, this interpretation does not explain the influence of oxygen and can not describe this XES structure. Therefore, the interpretation of this spectrum took into account the fact that the Th6p levels in  $\text{ThO}_2$  are not core and take an active part in IVMO formation [1, 3].

In the considered XES from  $\text{ThO}_2$ , the low energy wide band is poorly resolved, although the device resolution enables us to see the calculated peaks in the energy range of 60-76 eV (fig. 3; tab. 3). It can be partially explained by extra transitions not listed in tab. 3.

The  $\text{ThO}_2$  XES exhibits seven peaks in the energy range of 63.5-78.0 eV and a sharp peak at 80.7 eV. Taking into account the considered suggestions, one can come to the conclusion that the peaks in the energy range of 63.5-78.0 eV can be attributed to transitions from the IVMO, the sharp one – to the transition from the OVMO to the Th5d level (fig. 3, tab. 3). According to the dipole selection rules ( $\Delta l = 1$  and  $\Delta j = 0; 1$ ), a hole on the Th5d level can be filled with a p- or an fOVMO electron. It agrees with calculation results [1, 18] which indicate that the O2p states contribute significantly to the OVMO, aside from the contribution of Th5f states. This consideration is reasonable only in the approximation that the MO electrons maintain their partial atomic nature. The considered spectrum does not allow us to conclude ambiguously about the contribution of Th5f to OVMO.

During  $\text{ThO}_2$  XES formation, the initial state of the system with a hole on the Th5d level transits into the final state with a hole on one of the MOs, while during  $\text{ThO}_2$  XPS formation, the initial state without any holes transits into the final state with a hole on the core level. Therefore, energy schemes for these two processes are different and the comparisons of the XPS and XES in this work are rough (tab. 3). Further-

more, more detailed and precise calculations are required.

The obtained data shows that the  $O_{4,5}(\text{Th})$  XES from  $\text{ThO}_2$  can be interpreted only taking into account effective IVMO formation, in particular, with the participation of the relatively deep filled Th6p and O2s AOs.

We would like to note that, for the first time, this work studied the fine, low energy (0-40 eV) XPS and  $O_{4,5}(\text{Th})$  XES from  $\text{ThO}_2$  and established the correlation of the fine OVMO (0 – ~13 eV) and IVMO (~13~40 eV) related spectral structure parameters with the possible participation of Th5f electronic states in the formation of chemical bonds.

Practically, on the basis of  $O_{4,5}(\text{Th})$  XES and taking into account the fine XPS structure parameters, an experimental confirmation of IVMO formation in  $\text{ThO}_2$  has been achieved [3].

## CONCLUSIONS

1. Taking into account the  $\text{RX}_\alpha$ -DVM results for the  $\text{ThO}_8^{12-}(\text{D}_{4h})$  cluster, a quantitative interpretation of fine XPS outer valence (0-13 eV) and inner valence (13-40 eV) electronic structure in  $\text{ThO}_2$  was done for the first time.

1.1. Although thorium does not have Th5f electrons, filled Th5f electronic states (~0.6 Th5f electrons) in the outer valence band of  $\text{ThO}_2$  were shown to appear during the formation of the chemical bond.

1.2. Th6p electrons were shown to be a significant (experimentally observed) part (~0.44 Th6p electrons) of not only IVMO, but of OVMO formation as well. The most significant roles in the formation of IVMO in  $\text{ThO}_2$  were established to belong to Th6p<sub>3/2,1/2</sub> and O2s AOs of the neighboring Th and O ions.

1.3. IVMO composition and the sequent order in  $\text{ThO}_2$  was established in the binding energy range of 13 eV to 40 eV. The valence electronic state density in the range of 0-40 eV in  $\text{ThO}_2$  was calculated. Thus, for the bonding  $15\gamma_6$ ,  $11\gamma_7$  (7) and the antibonding  $17\gamma_6$ ,  $13\gamma_7$  (4) the calculation found out (14% of Th6p<sub>3/2</sub> + 84% of O2s and 76% of Th6p<sub>3/2</sub> + 10% of O2p), while for the bonding  $14\gamma_6$  (8) and antibonding  $16\gamma_6$  (5) the calculation found out (82% of Th6p<sub>1/2</sub> + 15% of O2s and 16% of Th6p<sub>1/2</sub> + 80% of O2s + 4% of Th7p).

2. For the first time, these data for the  $\text{ThO}_8^{12-}(\text{D}_{4h})$  cluster allowed an interpretation of the fine XPS (0-40 eV) and high resolution  $O_{4,5}(\text{Th})$  XES spectral structure (~60~85 eV) of  $\text{ThO}_2$ . This structure was shown to be formed with the OVMO (0~13 eV) and the IVMO (~13~40 eV) electrons. Practically, one more experimental evidence of IVMO formation from Th6p and O2s AOs in  $\text{ThO}_2$  was obtained.

## ACKNOWLEDGEMENT

The work was supported by the RFBR grants 08-03-00314 and 06-08-00808 and the State Program for Leading Scientific Schools, grant NSh-616.2008.3.

## REFERENCES

- [1] Teterin, Yu. A., Baev, A. S., Gagarin, S. G., Klimov, V. D., Structure of Photoelectron Spectra of Thorium Compounds (in Russian), *Radiohimiya*, 27 (1985), 1, pp. 3-13
- [2] Teterin, Yu. A., Teterin, A. Yu., Structure of X-Ray Photoelectron Spectra of Light Actinide Compounds, *Russian Chemical Reviews*, 73 (2004), 6, pp. 541-580
- [3] Teterin, Yu. A., Gagarin, S. G., Inner Valence Molecular Orbitals in Compounds and the X-Ray Photoelectron Spectra Structure (in Russian), *Russian Chemical Reviews*, 65 (1996), pp. 825-847
- [4] Makarov, L. L., Karaziya, H. I., Batrakov, Yu. F., Chemical Effects in the L-Spectra of Th. The Signs of Existence of the Bound 5f- State in Th Compounds (in Russian), *Radiohimiya*, 20 (1978), 1, pp. 116-124
- [5] Teterin, Yu. A., Teterin, A. Yu., The An5f-States of Actinides (Th, U, Np, Pu, Am, Cm, Bk) in Compounds and Parameters of Their X-Ray Photoelectron Spectra (in Russian), *Condensed Media and Interphase Borders*, 2 (2000), 1, pp. 60-66
- [6] Gubanov, V. A., Rosen, A., Ellis, D. E., Electronic Structure of Mono- and Dioxides of Thorium and Uranium, *J. Inorg. Nucl. Chem.*, 41 (1979), pp. 975-986
- [7] Teterin, Yu. A., Terekhov, V. A., Teterin, A. Yu., Utkin, I. O., Lebedev, A. M., Vukchevich, L., Inner Valence Molecular Orbitals and the X-Ray O<sub>4,5</sub>(Th)-Emission Spectra Structure in ThO<sub>2</sub> and ThF<sub>4</sub> (in Russian), DAN (Reports of the Russian Academy of Science), 358 (1998), 5, pp. 637-640
- [8] Veal, B. W., Lam, D. J., Diamond, H., Hoekstra, H. R., X-Ray Photoelectron Spectroscopy Study of Oxides of the Transuranium Elements Np, Pu, Am, Cm, Bk and Cf, *Phys. Rev.*, 15 (1977), 6, pp. 2929-2942
- [9] Shirley, D. A., High-Resolution X-Ray Photoelectron Spectrum of the Valence Bands of Gold, *Phys. Rev. B.*, 5 (1972), 12, pp. 4709-4714
- [10] Keller, C., Thorium, Verbindungen mit Edelgasen, Wasserstoff, Sauerstoff, Gmelin Handbuch der Anorganischen Chemie, Teil C1, Springer, Berlin-Heidelberg-New York, 1978
- [11] Rosen, A., Ellis, D. E., Relativistic Molecular Calculations in the Dirac-Slater Model, *J. Chem. Phys.*, 62 (1975), 8, pp. 3039-3049
- [12] Adachy, H., Relativistic Molecular Orbital Theory in the Dirac-Slater Model, *Technol. Reports Osaka Univ.*, 27 (1977), 1364-1393, pp. 569-576
- [13] Gunnarsson, O., Lundqvist, B. I., Exchange and Correlation in Atoms, Molecules and Solids by the Spin-Density-Functional Formalism, *Phys. Rev. B.*, 13 (1976), pp. 4274-4298
- [14] Pyykko, P., Toivonen, H., Tables of Representation and Rotation Matrices for the Relativistic Irreducible Representations of 38 Point Groups, *Acta Academiae Aboensis, B*, 43 (1983), 2, pp. 1-50
- [15] Varshalovich, D. A., Moskalev, A. N., Hersonsky, V. K., Quantum Theory of Angular Moment, Nauka, Leningrad, 1975
- [16] Slater, J. C., Johnson, K. H., Self-Consistent-Field X Cluster Method for Polyatomic Molecules and Solids, *Phys. Rev. B*, 5 (1972), 3, pp. 844-853
- [17] Band, I. M., Kharitonov, Yu. I., Trzhaskovskaya, M. B., The Photoionization Cross-Sections and Angular Distributions, *Atomic Data and Nuclear Data Tables*, 23 (1979), pp. 443-505
- [18] Gubanov, V. A., Rosen, A., Ellis, D. E., Electronic Structure and Bonding in ThO<sub>2</sub> and UO<sub>2</sub>, *Sol. State Commun.*, 22 (1977), 4, 975-986, pp. 219-223
- [19] Huang, K. N., Aojogi, M., Chen, M. N., Graseman, B., Mark, H., Neutral Atom Electron Binding Energies from Relaxed-Orbitals Relativistic Hartree-Fock-Slater Calculations, *Atom. Data and Nucl. Data Tables*, 18 (1976), pp. 243-291
- [20] Fugle, J. S., Burr, A. F., Watson, L. M., Fabian, D. Y., Lang, W., X-Ray Photoelectron Studies of Thorium and Uranium, *J. Phys. F: Metal. Phys.*, 4 (1974), 2, pp. 335-342
- [21] Teterin, Yu. A., Terekhov, V. F., Teterin, A. Yu., Utkin, I. O., Lebedev, A. M., Vukchevich, L., The Structure of the X-Ray Photoelectron and X-Ray Emission Spectra of ThO<sub>2</sub> and ThF<sub>4</sub> Related to the Electrons of Molecular Orbitals (in Russian), *J. of Struct. Chemistry*, 39 (1998), 6, pp. 1052-1054
- [22] Lyahovskaya, I. I., Ipatov, V. M., Zimkina, T. M., The Long-Wave X-Ray 5d Spectra of Thorium and Uranium in Compounds with Oxygen and Fluorine (in Russian), *J. of Struct. Chemistry*, 18 (1977), 4, pp. 668-672

**Антон Ј. ТЕТЕРИН, Михаил В. РИЖКОВ, Јуриј А. ТЕТЕРИН, Лабуд ВУКЧЕВИЋ,  
Владимир А. ТЕРЕХОВ, Константин И. МАСЛАКОВ, Кирил Е. ИВАНОВ**

### **ГУСТИНА ВАЛЕНТНИХ ЕЛЕКТРОНСКИХ СТАЊА У ТОРИЈУМДИОКСИДУ**

У раду се анализирају фини нискоенергетски (0-40 eV) рендгеном индуковани фотоелектронски спектри  $\text{ThO}_2$  са релативистичким прорачуном X –дискретних варијација електронске структуре  $\text{ThO}_8^{12-}(\text{D}_{4h})$  кластера који одражава торијумово блиско окружење у  $\text{ThO}_2$ . Као резултат, теоријски је показано и експериментално потврђено да Th5f електрони у  $\text{ThO}_2$  могу директно да учествују ( 0.6 Th5f електрона) у образовању хемијских веза. Показано је такође да су Th6p електрони део ( 0.44 Th6p електрона) не само унутрашњих валентних молекуларних орбитала већ да имају значајну улогу и у формирању спољашњих валентних молекуларних орбитала. Установљено је да композиција и редослед унутрашњих валентних молекуларних орбитала припадају енергијама везе у опсегу од 13 eV до 40 eV. Такође је израчуната густина валентних електронских стања у опсегу од 0 eV до 40 eV у  $\text{ThO}_2$ . По први пут, ови подаци омогућавају тумачење финих рендгеном индукованих фотоелектронских спектра (0-40 eV) и рендгеном индуковану емисиону спектралну структуру  $\text{O}_{4,5}(\text{Th})$  високе резолуције (~60 – ~85 eV)  $\text{ThO}_2$ .

*Кључне речи: рендген-индукована фотоелектронска спектроскопија, торијумоксид, спољашње и унутрашње валентне молекуларне орбитале*

---